

Collision-induced electronic quenching of aluminum monoxide

A.P. Salzberg, David I. Santiago, Federico Asmar, Deig N. Sandoval¹ and Brad R. Weiner²

Department of Chemistry, University of Puerto Rico, Río Piedras, PR 00931, USA

Received 11 October 1990; in final form 25 February 1991

Pulsed laser vaporization–laser-induced fluorescence has been used to produce $\text{AlO}(\tilde{B}^2\Sigma^+)$. Electronic quenching cross-sections for $\text{AlO}(\tilde{B}^2\Sigma^+, v' = 1)$ were determined by examining fluorescence decay rates in the presence of eight atomic and diatomic collision partners. The measured electronic quenching cross-sections extend from 0.2 to 14 \AA^2 . Some possible molecular mechanisms rationalizing the observed quenching cross-sections are discussed.

1. Introduction

A better understanding of the chemistry of small metal-containing molecules is fundamental to our comprehension of homogenous catalysis and activation of small molecules [1]. Metal oxides are one class of compounds that may be important intermediates in catalytic systems, yet the reaction dynamics of gas phase diatomic metal oxides have not been studied extensively, primarily because of the difficulty in producing them cleanly. Previous methods have included high-temperature ovens [2], shock tubes [3], exploding wires [4], flames [5] and flow reactors [6] to produce gas phase metal atoms, which have been subsequently oxidized. Recently, the use of focused lasers has been exploited to produce metal atoms by either multiphoton dissociation of organometallic compounds [7] or by laser vaporization of pure metals [8]. The metal atoms are allowed to react with an appropriate oxygen source, e.g. O_2 , N_2O , or CO_2 , to form the diatomic metal oxide, which can then be studied.

Aluminum monoxide, AlO , can be found in several high-temperature gas phase environments, such as rocket exhausts and explosives [9]. Its spectroscopic bands in the blue-green portion of the spec-

trum have been known for some time [10], and the physical properties of the molecule, such as its dissociation energy [11] and large dipole moment [12] have attracted quite a bit of attention. Fontijn and co-workers have studied the reactivity of ground state AlO towards Cl_2 [13], HCl [13], O_2 [2] and CO_2 [2] in a high-temperature fast-flow reactor. The results of these experiments provide evidence that AlO tends to efficiently abstract atoms, i.e. Cl or O , from small molecules at high temperature, even though other exothermic reaction pathways exist. Parnis et al. [7] have found the opposite behavior for room temperature reactions, i.e., that AlO prefers to form association complexes with electron donor molecules.

Several diatomic hydrides, i.e. OH [14], CH [15], NH [16], and BH [17], and the non-hydride, NF [18], have been studied extensively with respect to electronic quenching by an assortment of molecules. A variety of effects have been found to be important in this quenching process, such as the electrostatic moments, geometry, mass and the proton affinity of the quencher, and the rotational and kinetic energy content of the species to be quenched. Efficient electronic quenching is usually explained by postulating the formation of a collision complex, where energy can flow freely. AlO poses an interesting case study for electronic quenching experiments for the following reasons. First, its large dipole moment may cause strong attractive forces that can lead to efficient complex formation, and hence, collisional quenching. Second, is the tendency of ground state AlO to

¹ To whom correspondence should be addressed.

² Present address: Department of Chemistry, University of Texas-Pan American, 201 West University Drive, Edinburg, TX 78539-2999, USA.

wards abstraction reactions [2,13], i.e. to not form collision complexes, at high temperature, but to form associations with electron donor molecules at room temperature [7]. These effects present an interesting experimental challenge.

We report here our results of the dynamics of AlO in the $\tilde{B}^2\Sigma^+$ electronic state with helium and seven different diatomic collision partners. Collision-induced quenching of AlO is studied here by using the laser vaporization–laser-induced fluorescence technique, i.e. production of metal atoms by pulsed laser vaporization of a bulk metal which are allowed to react with an oxidizer, followed by resonant, pulsed laser excitation of the metal oxide product at some variable delay time. Electronic quenching cross-sections are then determined from the fluorescence lifetimes in the presence of different collision partners. These studies represent, to the best of our knowledge, the first quantitative measurements of electronic quenching cross-sections in an open-shell metal oxide with quenchers other than helium.

2. Experimental

A schematic of the experimental apparatus is shown in fig. 1. A six-way stainless steel cross (2.5" diameter), fitted with 18" long brass extension arms, serves as the reaction chamber for this experiment. The cell is evacuated by a mechanical vacuum pump through one arm of the cross, and pressures are measured at the exit point by a Baratron capacitance ma-

nometer. The brass arm extensions have Suprasil quartz windows mounted on O-ring seals at Brewster's angle, and contain two cone-shaped light baffles on each side to minimize scattered laser light. Aluminum atoms are produced by laser vaporization of a 1" \times 1" \times 0.25" aluminum flat mounted on the shaft of a rotary motion feedthrough with an adjustable nylon coupler. In order to prevent drilling a hole in the aluminum flat by the vaporization laser, the shaft is slowly rotated (\approx 6 rpm) by an externally mounted motor. If the sample is not rotated, the shot-to-shot fluctuations are large, and eventually the signal disappears altogether as a hole is drilled in the metal. The vaporization laser for all the reported data was the 355 nm output of a Nd:YAG laser (Quantel YG581C; pulsewidth \approx 10 ns), but we have been able to generate Al atoms with the 532 nm output of the same Nd:YAG laser, or with a KrF (248 nm) excimer laser. In all cases, the vaporization laser is focused to a point onto the aluminum surface with a 150 mm focal length Suprasil quartz lens, whose position is accurately controlled with an adjustable lens positioner. Laser fluences of 300 mJ/cm² at 355 nm (prior to focusing) are possible with our laser system, but we find too much background emission is produced at these laser energies, and therefore, we typically work between 150 and 200 mJ/cm². AlO is produced when the laser vaporization is carried out in the presence of O₂ (0.05–20 Torr), and is detected by laser-induced fluorescence (LIF) of the $\tilde{B}-\tilde{X}$ (1, 0) transition near 465 nm. The probe laser is a Lambda Physik FL 3002 tunable dye laser pumped by a XeCl excimer laser (Lambda Physik LPX 205i; pulsewidth \approx 20 ns) operating at 308 nm. The dye laser beam is directed down the length of the cell, and passes within 2 mm of the rotating flat and intersects the focused vaporization laser. The AlO fluorescence signal is found to be dependent on where the focal point of the vaporization laser lies, and on a good spatial overlap of the two laser beams. The fluorescence is observed with a Hamamatsu R943-02 photomultiplier, at 90° relative to both the probe and the vaporization lasers, through a sapphire window. The emission is passed through a series of cut-off filters to minimize the scatter of the vaporization laser off the metal surface, and a bandpass filter centered on the (1, 1) and (0, 0) transitions of the $\tilde{B}-\tilde{X}$ band, to reduce dye laser scatter. The dye laser can

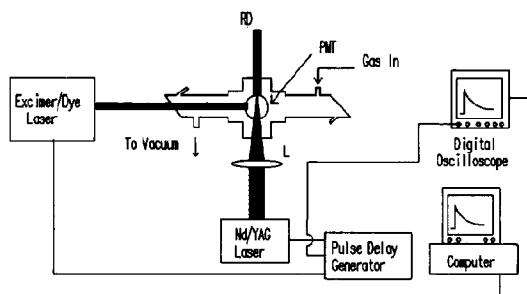


Fig. 1. Schematic diagram of the experimental apparatus used in the laser vaporization/laser-induced fluorescence studies; RD=rotating disk; PMT=photomultiplier tube; L=lens. See text for further explanation.

be fired at variable delay times relative to the vaporization laser by using a Stanford Research Systems DG535 digital delay pulse generator. All of the data reported here have been obtained at a delay time of 20 μ s. Typical shot-to-shot fluctuations of the fluorescence signal are 10–20%. Collision-induced quenching measurements are made as a function of added quencher gas, M, pressures. The gases are added through an inlet in one of the brass arms, and all experiments are done under static fill conditions.

Experiments have also been performed where the emission spectrum following the laser vaporization of aluminum in the presence of O₂ has been resolved through a 0.22 m double monochromator (Spex 1680B). The output of the photomultiplier is signal averaged either with a gated integrator (Stanford Research Systems SR250)/microcomputer (Northgate 286) system for spectroscopic identification or by a 350 MHz digital storage oscilloscope (LeCroy model 9420) for the fluorescence lifetime measurements. The temporal resolution of the oscilloscope used for these experiments is 10 ns. Typically, 100 transients are averaged for the lifetime measurements (see fig. 2). The data obtained on the digital storage oscilloscope is transferred to the microcomputer for analysis and data storage. Logarithms of the decays are taken and fit by a linear least-squares routine. To avoid contributions due to the instrumental risetime, the first 70 ns of the fluorescence signal is not used in the linear least-squares fits. The decays were fit over 2–3 radiative lifetimes with uncertainties of less than 10%.

Aluminum samples were taken from standard plates. The suppliers and the stated purities of the gases used were: helium (General Gases; 99.995%), oxygen (General Gases; 99.99%), carbon monoxide (Matheson; 99.5%), chlorine (Matheson; 99.5%), hydrogen (Matheson, 99.99%), hydrogen bromide (Matheson, 99.8%), hydrogen chloride (Matheson; 99.0%), and nitrogen (General Gases; 99.998%). All gases were used as purchased from the supplier.

3. Results

3.1. Production of AlO

Laser vaporization of aluminum metal at 355 nm in the presence of small amounts of oxygen leads to

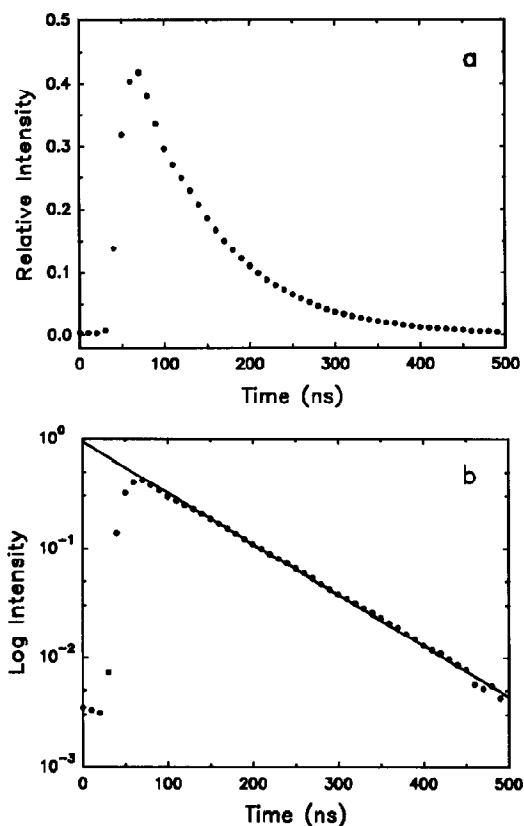


Fig. 2. (a) Typical fluorescence decay of the AlO($\tilde{B}^2\Sigma^+$) state. (b) Plot of the logarithm of the AlO($\tilde{B}^2\Sigma^+$) fluorescence decay. The straight line is a linear least-squares fit to the data.

the production of aluminum oxide. We have observed the direct production of both AlO($\tilde{B}^2\Sigma^+$) by emission spectroscopy and AlO($\tilde{X}^2\Sigma^+$) by laser-induced fluorescence (LIF) spectroscopy. By using emission spectroscopy we have directly observed several transitions from excited states of Al near 395 nm ($4^2S \rightarrow 3^2P_{1/2,3/2}$) and 308 nm ($3^2D_{3/2,5/2} \rightarrow 3^2P_{1/2,3/2}$) from the laser vaporization of aluminum metal with no oxygen present [19]. A small peak was detected at ≈ 365 nm, which we tentatively assigned to the ($\tilde{E}^3\Sigma_g \rightarrow \tilde{X}^3\Pi$) transition of the aluminum dimer [20]. Our attempts to look for Al₂ by LIF on this same transition were unsuccessful. The addition of oxygen to the cell during the laser vaporization at 355 nm produces an intense blue-green flame on top of the metal surface, which we attribute to the AlO

($\tilde{B}-\tilde{X}$) transition. This observation is confirmed by the appearance of two broad bands in the emission spectrum with bandheads near 465 and 488 nm. The presence of $\text{AlO}(\tilde{X}^2\Sigma^+)$ has been confirmed by measuring the LIF excitation spectrum on the $\tilde{B}-\tilde{X}$ transition, which agrees with the literature [21]. In the absence of O_2 , no LIF signal was observed.

In order to produce the $\text{AlO}(\tilde{B}^2\Sigma^+)$ for the collisional quenching studies, we allow the excited AlO to relax and thermalize over a delay time (10–50 μs) and then excite the AlO on the 1, 0 bandhead of the $\tilde{B}-\tilde{X}$ transition at 464.8 nm. The decay (see fig. 2) of the fluorescence is then monitored as a function of added gas.

3.2. Quenching studies of $\text{Al}(\tilde{B}^2\Sigma^+)$

The lifetime of $\text{AlO}(\tilde{B}^2\Sigma^+)$ has been measured here by a standard Stern–Volmer analysis, where the intercept, i.e. zero pressure of quencher gas, of the fluorescence decay rates versus $[\text{M}]$ gives the $1/\tau$ value, where τ is the radiative lifetime. Fig. 3 shows the standard analysis for three different collision partners. Within the reported errors, there is no evidence for curvature in the Stern–Volmer plot. If we take an average of our intercept values (see fig. 3) for the different quencher gases, we obtain a radiative lifetime of 97 ± 12 ns for the $v' = 1$ level of the $\text{AlO}(\tilde{B}^2\Sigma^+)$ electronic state. Upon addition of other collision partners, M , we observe an increase in the

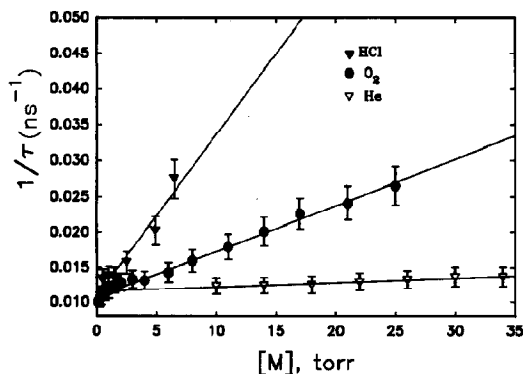


Fig. 3. Stern–Volmer plot of the $1/\tau$ (ns^{-1}) for three different quencher gases used. The error bars represent a 1σ statistical error taken from the data collected at each pressure, and the straight lines are linear least-squares fits to the data points.

Table 1

Quenching rate constants, $k_{\text{Q,M}}$ ($\text{M} = \text{quencher}$), in $10^{-12} \text{ cm}^3 \text{ molecule}^{-1} \text{ s}^{-1}$ and quenching cross-sections, $\sigma_{\text{Q,M}}$, in \AA^2 for the $\tilde{B}^2\Sigma^+$ ($v' = 1$) state of AlO at 298 K, and reaction cross-section, σ_{reaction} in \AA^2 , for the $\tilde{X}^2\Sigma^+$ of AlO at 298 K

M	$k_{\text{Q,M}}$	$\sigma_{\text{Q,M}}$	$\sigma_{\text{reaction}}^{\text{a)}}$
He	2.86 ± 0.29	0.22 ± 0.02	
H_2	14.11 ± 2.33	0.78 ± 0.13	$< 0.001^{\text{b)}$
N_2	20.01 ± 5.46	3.27 ± 0.89	
O_2	21.12 ± 0.74	3.60 ± 0.13	$0.85^{\text{c)}$
CO	7.78 ± 0.53	0.81 ± 0.06	$0.05^{\text{b)}$
Cl $_2$	35.16 ± 3.49	7.24 ± 0.72	$0.94^{\text{c)}$
HCl	69.74 ± 6.70	12.42 ± 1.19	$6.23^{\text{c)}$
HBr	34.11 ± 9.39	7.20 ± 1.98	

^{a)} Cross-sections for ground state reactions of $\text{AlO} + \text{M}$ calculated from rate constants of the references listed by use of eq. (1).

^{b)} Ref. [1]. ^{c)} Refs. [2,13].

rate of fluorescence decay. The bimolecular quenching rate constants, $k_{\text{Q,M}}$, for different colliders are given in table 1. The reported errors are 1σ .

Bimolecular quenching rates can be converted into cross-sections, which gives values that are corrected for the relative velocities of the colliding molecular pair. The experimental quenching rate constants are converted by the relation,

$$\sigma_{\text{Q,M}} = (\pi\mu/8k_{\text{B}}T)^{1/2}k_{\text{Q,M}}, \quad (1)$$

where μ is the reduced mass of the AlO quencher pair, k_{B} is the Boltzmann constant, and T is the temperature in K. The cross-sections and their errors (1σ) are reported in table 1.

4. Discussion

The fluorescence lifetime of $\text{AlO}(\tilde{B})$ has been previously measured by Johnson et al. to be 125.5 ± 2.6 ns for $v' = 1$ [22] and later by Dagdigian et al., who reported a value of 102 ± 7 ns for the same vibrational level of the excited state [21]. Our average measured lifetime value confirms within experimental error, the latter value. Our measured lifetime value may be slightly low, due to the presence of small amounts of O_2 used to produce AlO , which may subsequently quench the fluorescence. To verify our average lifetime, we have measured the fluorescence lifetime at the smallest amount of O_2 (0.11 Torr)

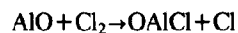
pressure, where we can still obtain a good signal-to-noise ratio (see fig. 3). In this case, we obtained a fluorescence lifetime of 100 ± 17 ns, which agrees with the averaged value.

The experimental quenching rates measured here monitor only the total rate of decay of the $\text{AlO}(\tilde{\text{B}}^2\Sigma^+, v'=1)$ species. No distinction can be made a priori between non-reactive and reactive collisions. Johnson et al. have reported that the $\text{AlO}(\tilde{\text{B}}^2\Sigma^+)$ fluorescence signal was independent of the added gases He (0.25–50 Torr), N_2 (0.8–20 Torr) and O_2 (0.01–10 Torr) [22]. Our results (see fig. 3 and table 1) show that there is, in fact, a decrease in the fluorescence lifetimes in the presence of added collider gases. In order to understand these changes in the fluorescence lifetime, we must be able to examine the possible fates of $\text{AlO}(\tilde{\text{B}}^2\Sigma^+)$. Since we are measuring the decay of a vibrationally excited species, we must first consider the possibility of vibrational relaxation as the decay mechanism. The quenching rates observed in this study are 1–2 orders of magnitude higher than those typically observed for collision-induced vibrational relaxation [23]. Furthermore, if the $\text{AlO}(\tilde{\text{B}}^2\Sigma^+, v'=1)$ would relax to $\text{AlO}(\tilde{\text{B}}^2\Sigma^+, v'=0)$ prior to emission, we would still observe fluorescence of a similar lifetime [21], since our bandpass filter is centered on $\Delta v=0$ transition of the B–X system.

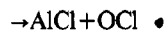
One possible pathway for the quenching rates measured here for $\text{AlO}(\tilde{\text{B}}^2\Sigma^+)$ is that they can be due to excited state reactions. This is unlikely for some of the more inert species studied (He, N_2), but may be possible for some others. The reaction rates of $\text{AlO}(\tilde{\text{X}}^2\Sigma^+)$ with HCl, O_2 , CO and H_2 have been determined [2,7,13]. One way to judge the feasibility of excited state reactions as the quenching mechanism, is to compare the electronic quenching cross-section with the ground state reaction cross-section. If the values are comparable, then it is very likely that the quenching may be due to excited state reactions [18]. This is a valid assumption in the case of AlO because both the $\tilde{\text{B}}$ and $\tilde{\text{X}}$ states have the same electronic symmetry, and will therefore correlate with the same product channels. For the case where the quenching cross-section is several orders of magnitude greater than the ground state reaction cross-section, some type of physical quenching remains a more plausible explanation. While this model may be sim-

plistic, it provides a good starting point towards determining the mechanism by which quenching occurs. In order to obtain cross-sections for AlO ground state reactions with O_2 , Cl_2 , and HCl at 298 K, we must assume that the Arrhenius plots of Fontijn and co-workers can be extrapolated linearly [2,13]. If so we can obtain bimolecular rate constants at 298 K and thus the reaction cross-sections for $\text{AlO}(\tilde{\text{X}}^2\Sigma^+) + \text{O}_2$, Cl_2 , and HCl are 0.85, 0.94 and 6.23 \AA^2 , respectively. These values are summarized in table 1. For the case of comparison with ground state AlO reactions with H_2 and CO, we use the 298 K rate data of Parnis et al., which give reaction cross-sections of <0.001 and 0.05 \AA^2 , respectively [7]. A comparison of these cross-sections reveals that they are comparable (within an order of magnitude) for the O_2 , Cl_2 and HCl cases, but are less comparable for the CO (different by a factor of 25) and H_2 ($1000\times$ different) cases.

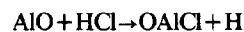
While it may be speculative to assume that excited state reactions are the quenching mechanism for $\text{AlO}(\tilde{\text{B}}^2\Sigma^+)$ fluorescence, we would like to illustrate some of the possibilities. For the ground state AlO reactions with Cl_2 and HCl, consider the following pathways:



$$\Delta H_{298}^0 = -294 \text{ kJ mol}^{-1}, \quad (2)$$



$$\Delta H_{298}^0 = -17 \text{ kJ mol}^{-1}, \quad (3)$$



$$\Delta H_{298}^0 = -105 \text{ kJ mol}^{-1}, \quad (4)$$



$$\Delta H_{298}^0 = -33 \text{ kJ mol}^{-1}, \quad (5)$$



$$\Delta H_{298}^0 = +13 \text{ kJ mol}^{-1}. \quad (6)$$

Due to the absence of any LIF signal from AlCl, Slovejkov et al. believe that the decay of $\text{AlO}(\tilde{\text{X}}^2\Sigma^+)$ is occurring by the abstraction mechanisms, reactions (2) and (4) (and possibly (5)) [13]. For the case of the excited state reactions, the same channels are thermochemically allowed, but are now more exothermic by the photon energy, $E=h\nu=261.9 \text{ kJ/}$

mol. Eq. (6) is the only new reaction pathway that becomes thermochemically allowed as a result of the added photon energy. Because of the similarity of the quenching cross-sections of both Cl_2 and HCl , and also with the reactive cross-sections of the ground state, it is very likely that excited state reactions (by one of the above mechanisms) could be the quenching pathway.

Similar reaction schemes can be drawn for the $\text{AlO}(\tilde{\text{B}}^2\Sigma^+) + \text{CO}$, HBr and even H_2 cases, but we believe it is not fruitful to consider these cases when there is so little known about the ground state reactions. The only definitive method of proving these reaction channels is to directly measure the proposed products.

For the cases of non-reactive quenching, arising from energy transfer during collisions with inert species, e.g. He , the mechanism remains unclear. Several possibilities exist: (1) The $\text{AlO}(\tilde{\text{B}}^2\Sigma^+)$ electronic energy is directly converted into translational energy through collisions with He , and (2) the AlO molecule in the $(\tilde{\text{B}}^2\Sigma^+)$ state is collisionally transferred into some other overlapping electronic state (e.g. $\text{AlO}(\tilde{\text{A}}^2\Pi)$). In the first case, a single exponential decay would be observed, as is seen in our experiments. The second case could result in competitive and/or reversible pathways, and the observed decay may no longer be consistent with a single exponential process. For example, the overlapping electronic state could also emit back to the ground state. However, due to our simple detection system, consisting of a photomultiplier and filters, we are most likely blocking out secondary emission.

By measuring the vibrational level dependence of the collisional quenching cross-sections, some of these mechanisms could be differentiated. For the case of $\text{BaO}(\tilde{\text{A}}^1\Sigma^+)$, Johnson has measured the cross-sections of electronic quenching with helium as the collision partner [24]. The measured quenching cross-sections were found to vary with vibrational level from 0.28 to 2.49 \AA^2 . The variance with vibrational level was explained by collisional transfer of the BaO into a perturbing state. A similar explanation may apply here for our similar cross section value of $\text{AlO} + \text{He}$. The fate of $\text{AlO}(\tilde{\text{B}}^2\Sigma^+)$ could very easily be to higher vibrational levels of the $\text{AlO}(\tilde{\text{A}}^2\Pi)$ state, which has an origin about 15000 cm^{-1} below the B state, or to other higher multiplet states of AlO .

The experiments reported in this paper represent the first use of the pulsed laser vaporization technique in measuring fluorescence lifetimes and electronic quenching cross sections. The technique greatly simplifies the previous methods of producing gas phase diatomic metal oxides, and enables us to study the dynamics of a wide range of metal oxides, metal halides, and other metal-containing species. The detailed mechanisms of the collision-induced quenching of $\text{AlO}(\tilde{\text{B}}^2\Sigma^+)$ are still not resolved. Further experimental and theoretical work is ongoing to elucidate these mechanisms [25].

Acknowledgement

The experiments reported here were conducted in the Puerto Rico Laser and Spectroscopy Facility, which is co-sponsored by NSF-EPSCoR (Grant No. R11-8610677) and NIH-RCMI (Grant No. RR03541). We would also like to kindly acknowledge the partial support of the Naval Surface Warfare Center (Contract No. N60921-89-R-0220) and the Office of Naval Research (Grant No. N00014-89-J-1829). DNS acknowledges summer support from the NSF-CRCM program (Grant No. USE-8850605). We thank Herb Nelson for helpful discussions.

References

- [1] E.L. Muettterties and M.J. Krause, *Angew. Chem.* 95 (1983) 135.
- [2] A. Fontijn, *Spectrochim. Acta* 54B (1988) 1075.
- [3] A.M. Bass, N.A. Keubler and L.S. Nelson, *J. Chem. Phys.* 40 (1964) 3121.
- [4] B. Rosen, *Nature* 156 (1945) 570.
- [5] K.J. Kaufman, J.L. Kinsey, H.B. Palmer and A. Tewerson, *J. Chem. Phys.* 60 (1974) 4023.
- [6] J.B. West, R.S. Bradford, J.D. Eversole and C.R. Jones, *Rev. Sci. Instrum.* 46 (1975) 164.
- [7] J.M. Parnis, S.A. Mitchell, T.S. Kanigan and P.A. Hackett, *J. Phys. Chem.* 93 (1989) 8045.
- [8] D. Ritter and J.C. Weisshaar, *J. Phys. Chem.* 93 (1989) 1576.
- [9] C. Park, *Atmos. Environ.* 10 (1976) 693; R.A. Ogle, J.K. Beddow, L.D. Chen and P.B. Butler, *Combustion Sci. Technol.* 61 (1988) 75.

- [10] A. Gatterer, J. Junkes and E.W. Salpeter, *Molecular spectra of metallic oxides* (Specola Vaticana, Citta del Vaticano, 1957).
- [11] M. Costes, C. Naulin, G. Dorthe, C. Vauchamps and G. Nouchi, *Faraday Discussions Chem. Soc.* 84 (1987) 74, and references therein.
- [12] B.H. Lengsfeld and B. Liu, *J. Chem. Phys.* 77 (1982) 6083.
- [13] A.G. Slavejkov, C.T. Stanton and A. Fontijn, *J. Phys. Chem.* 94 (1990) 3347.
- [14] G.P. Smith and D.R. Crosley, *J. Chem. Phys.* 82 (1985) 4022, and references therein.
- [15] P. Heinrich, R.D. Kerner and F. Stuhl, *Chem. Phys. Letters* 147 (1988) 575, and references therein.
- [16] N. Garland and D.R. Crosley, *J. Chem. Phys.* 90 (1989) 3566, and references therein.
- [17] C.H. Douglass and J.K. Rice, *J. Phys. Chem.* 93 (1989) 7659.
- [18] K.Y. Du and D.W. Setser, *J. Phys. Chem.* 94 (1990) 2425.
- [19] C.E. Moore, *Atomic energy levels*, Vol. 1 (Nat. Bur. Std. US GPO, Washington, 1949).
- [20] M.F. Cai, T.P. Dzuga and V.E. Bondybey, *Chem. Phys. Letters* 155 (1989) 430.
- [21] P.J. Dagdigian, H.W. Cruse and R.N. Zare, *J. Chem. Phys.* 62 (1975) 1824.
- [22] S.E. Johnson, G. Capelle and H.P. Broida, *J. Chem. Phys.* 56 (1972) 663.
- [23] I.M. Campbell and D.L. Baulch, in: *Gas kinetics and energy transfer*, Vol. 3, eds. P.G. Ashmore and R.J. Donovan (The Chemical Society, London, 1978) pp. 66–81.
- [24] S.E. Johnson, *J. Chem. Phys.* 56 (1972) 149.
- [25] H. Wang, A.P. Salzberg, D.I. Santiago and B.R. Weiner, to be published.